

Thermoremanence and zero-field-cooled/field-cooled magnetization study of $\text{Co}_x(\text{SiO}_2)_{1-x}$ granular films

J. C. Denardin,¹ A. L. Brandl,¹ M. Knobel,¹ P. Panissod,² A. B. Pakhomov,³ H. Liu,⁴ and X. X. Zhang⁴

¹ *Instituto de Física “Gleb Wataghin,” UNICAMP, C.P. 6165, 13083-970, Campinas, S.P., Brazil*

² *Institut de Physique et Chimie des Matériaux de Strasbourg, 67 037 Strasbourg, France*

³ *Magnetics Innovation Center (MAGIC), MCPF, Hong Kong University of Science and Technology, Clear Water Bay, Kowloon, Hong Kong, China*

⁴ *Physics Department and Institute of Nanoscience and Technology (INST), Hong Kong University of Science and Technology, Clear Water Bay, Kowloon, Hong Kong, China*

(Received 28 April 2001; revised manuscript received 13 August 2001; published 18 January 2002)

A systematic study of $\text{Co}(\text{SiO}_2)$ granular films by means of transmission electron microscopy (TEM), dc and ac initial magnetic susceptibility, and thermoremanent magnetization (TRM) is presented. The experimental results are compared with simulations of zero-field-cooled (ZFC) and field-cooled (FC) magnetization and TRM curves obtained using a simple model of noninteracting nanoparticles. The simulated ZFC/FC curves, using the actual parameters obtained from the TEM images, show a different behavior than the experimental magnetic data. The effect of the dipolar interaction among particles introduces a self-averaging effect over a correlation length Λ , which results in a larger average “magnetic” size of the apparent particles together with a narrower size distribution. The analysis of the ZFC/FC curves in the framework of independent “particle clusters” of volume Λ^3 , involving about 25 real particles, explains very well the observed difference between the experimental data for the median blocking temperature $\langle T_B \rangle$ and their distribution width with respect to the ones expected from the structural observations by TEM. The experimental TRM curves also differ from those obtained from the theoretical model, starting to decrease at a lower temperature than expected from the model, also indicating the strong influence of dipole-dipole interactions.

DOI: 10.1103/PhysRevB.65.064422

PACS number(s): 75.20.-g, 75.50.Tt, 75.75.+a

I. INTRODUCTION

In addition to the fundamental importance of unresolved problems in basic magnetism, the study of nanocrystalline systems is more and more of practical importance, owing to the rapid approach to the so-called superparamagnetic limit on magnetic recording media. Granular magnetic systems have been studied since the 1950s, with a renewed interest after the discovery of giant magnetoresistance on Cu-Co films in 1992.^{1,2}

Several factors can influence the magnetic and magnetotransport behavior of granular systems, namely, the distribution of grain sizes, the shape of the grains, and the magnetic anisotropy of the individual grains. Also, it is well known that the interactions among magnetic particles play a dominant role in the physical properties of these systems. Although it has been studied very intensively, it remains unclear how the magnetic interactions affect the magnetic behavior of nanoscopic systems. Due to interactions the behavior of a magnetic moment is not only governed by its own intrinsic anisotropy energy E_a , but also by the coupling with its neighbors. The interplay between the dipolar interaction and the distribution of the energy barriers (sizes) will certainly modify the magnetic response of particles. When the interactions are strong enough, the particles may behave as a spin glass,^{3,4} although a true phase transition needs the combined effects of dipolar interaction and anisotropy.⁵

Several magnetic techniques are currently employed to indirectly infer the structural parameters and intrinsic magnetic properties. In addition to hysteresis loops that can be

fitted using properly weighted Langevin functions,⁶ the most used techniques are the so-called zero-field-cooled(ZFC)/field-cooled(FC) magnetization⁷ and thermoremanent magnetization (TRM),⁸ from which it is possible to extract information about the average blocking temperature (and therefore the mean grain diameter, if the particles considered are of spherical shape with a known anisotropy constant). The dispersion of grain sizes can be estimated from the difference between the maximum in the ZFC curve and the bifurcation between the ZFC and FC curves or from the fit of the TRM curve. Although these data are widely used to characterize nanocrystalline systems, it is worth noting that they should be employed with extreme care, because the dipolar interactions may cause strong deviations in the extracted structural parameters, although the shapes of the curves remain similar to the ones expected for noninteracting systems. In this paper we show a possible alternative to properly interpret the experimental data obtained in a cluster system in which interactions do play a very important role.

To achieve this task, we performed a systematic study of a $\text{Co}_{0.35}(\text{SiO}_2)_{0.65}$ granular film. This film belongs to a family of $\text{Co}_x(\text{SiO}_2)_{1-x}$ ($x=0.35, 0.41, \text{ and } 0.44$) films fabricated for the study of the giant Hall effect.^{9,10} This film is appropriate for our present work since it has a rather small magnetic particles concentration, well below the percolation limit, and the only possible magnetic interactions are of dipolar origin. From transmission electron microscopy (TEM) images, the real particle size distribution was obtained and well fitted by a log-normal distribution function. Magnetic properties, such as initial susceptibility and thermoremanent

magnetization, were measured as functions of T . The magnetic results are then compared with simulations of ZFC and FC magnetization and TRM curves with the particle size parameters obtained from the TEM images, using a simple model of noninteracting particles. Some hints about the possible effects of dipolar interactions are given in terms of the observed results.

II. THEORETICAL BACKGROUND

The Néel (Ref. 11) expression of the relaxation time of a superparamagnetic particle is $\tau = \tau_0 \exp(E_a/k_B T)$, where $E_a = KV$ denotes the particle's energy barrier separating the energy minima (uniaxial anisotropy), K and V are the magnetic anisotropy constant and the particle volume, respectively, k_B is the Boltzmann's constant, and T is the absolute temperature. The preexponential factor τ_0 (estimated to be $\approx 10^{-9} - 10^{-10}$ s) is a constant related to gyromagnetic precession.¹¹ The blocking temperature T_B , for a system of particles with mean volume V , is defined as the temperature at which $\tau = t_m$, the measurement time. At high temperatures the magnetic-moment relaxation time τ can be so small that the particles can rapidly achieve thermal equilibrium during the measurement time t_m . Therefore, when $T > T_B$, the system will behave as a "superparamagnet," while for $T < T_B$ the particles are said to be blocked, i.e., their magnetic moments remain at a fixed direction during a single measurement. The initial susceptibility for a single particle of volume V is given by¹² $\chi_{sp} = M_s^2 V / 3k_B T$ for $T > T_B$ and $\chi_{bl} = M_s^2 / 3K$ for $T < T_B$, where M_s is the saturation magnetization of the bulk material.

The ZFC magnetization curve is obtained after cooling the sample in zero field from high temperature by measuring the magnetization at stepwise increasing temperatures in a small applied field (20 Oe in the present case). The FC magnetization curve is obtained by measuring M in the cooling process in the same small applied field. In these experiments the typical measuring time t_m at each temperature was approximately 100 s. In any real fine particle system there is a distribution of particle sizes which gives rise to a distribution of blocking temperatures T_B . The initial susceptibility of such a system of noninteracting particles with a distribution of particle volumes and blocking temperatures is¹³

$$\chi_{ZFC} = \frac{M_s^2 \langle V \rangle}{3k_B T} \int_0^T \frac{T_B}{\langle T_B \rangle} f(T_B) dT_B + \frac{M_s^2}{3K} \int_T^\infty f(T_B) dT_B, \quad (1)$$

where $f(T_B)$ is the distribution function of blocking temperatures, $\langle V \rangle$ is an "average" volume, and $\langle T_B \rangle$ an "average" blocking temperature that are related through the Néel's expression for $t = t_m$. Actually, using this relationship between $\langle V \rangle$ and $\langle T_B \rangle$, Eq. (1) can be rewritten as

$$\chi_{ZFC}(T) = \frac{M_s^2}{3K} \left[\ln \left(\frac{t_m}{\tau_0} \right) \int_0^T \frac{T_B}{T} f(T_B) dT_B + \int_T^\infty f(T_B) dT_B \right]. \quad (2)$$

In Eqs. (1) and (2) the first term comes from the superparamagnetic particles whereas the second term comes from the blocked particles.

To model the FC susceptibility we use the same contribution from the superparamagnetic particles, but the contribution of the blocked particles to the magnetization is supposed to be that reached by the superparamagnetic particles in the small applied field at their blocking temperature. Thus, one can write the FC susceptibility as

$$\chi_{FC}(T) = \frac{M_s^2}{3K} \left[\ln \left(\frac{t_m}{\tau_0} \right) \int_0^T \frac{T_B}{T} f(T_B) dT_B + \ln \left(\frac{t_m}{\tau_0} \right) \int_T^\infty \frac{T_B}{T} f(T_B) dT_B \right], \quad (3)$$

i.e.,

$$\chi_{FC}(T) = \frac{M_s^2}{3K} \ln \left(\frac{t_m}{\tau_0} \right) \left[\frac{1}{T} \int_0^T T_B f(T_B) dT_B + \int_T^\infty f(T_B) dT_B \right]. \quad (4)$$

Again, the first term comes from the superparamagnetic particles while the second term is from the blocked ones.

To obtain TRM curves we have cooled the sample down to a low temperature in a high applied field (40 kOe in the present case), strong enough to saturate the sample, followed by magnetization measurements at increasing temperatures. At each temperature the sample was submitted to this high applied field for 60 s, the field was then switched off, and after a waiting time of 100 s the remanent magnetization was measured. Thus the remanent magnetization measured here is a measure of the magnetic-moment of all clusters that are still blocked at a given temperature for a time scale of $t_m \approx 100$ s. It therefore reflects the probability of finding clusters with a blocking temperature (T_B) higher than the measurement temperature T , i.e., the complementary partition function of the blocking temperatures.¹³ Then, the TRM can be expressed as

$$M_{TRM}(T)/M_s = 0 + \gamma \int_T^\infty f(T_B) dT_B, \quad (5)$$

where the factor γ is equal to the crystallographic orientational average of the blocked magnetic moments randomly distributed in a hemisphere ($\gamma = 0.5$ in the case of uniaxial anisotropy). Since the applied field is zero when the measurement is made, there is no contribution from the unblocked particles (the zero term was just inserted to stress that fact).

This simple model allows one to analyze the effect of various factors on the ZFC, FC, and TRM curves. One sees that, for noninteracting particles, the different kinds of measurements differ only by the prefactors. In particular the curve obtained from the difference between FC and ZFC curves should show similar temperature dependence to the TRM curve, and the derivatives with respect to temperature T of both curves parallel the distribution of blocking temperatures $f(T_B)$.

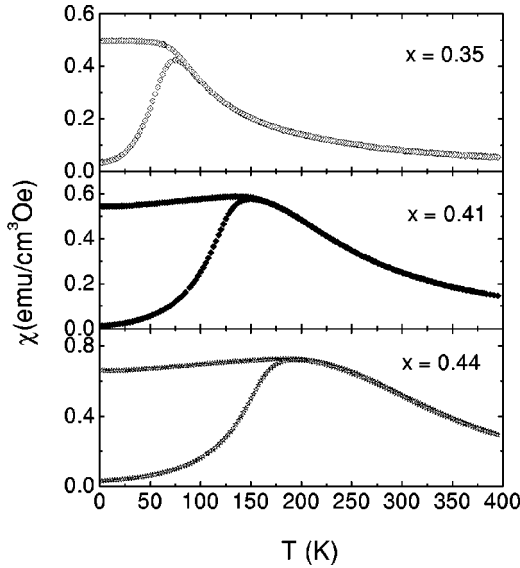


FIG. 1. Zero-field-cooled (ZFC) and field-cooled (FC) dc magnetic susceptibility, measured at 20 Oe for granular $\text{Co}_x(\text{SiO}_2)_{1-x}$ films with $x=0.35, 0.41,$ and 0.44 .

III. EXPERIMENT

The $1\text{-}\mu\text{m}$ thick granular $\text{Co}_x(\text{SiO}_2)_{1-x}$ films with metal volume fractions $x=0.35, 0.41,$ and 0.44 were prepared by cosputtering the cobalt and SiO_2 targets mounted on two separate guns. The glass substrates were held at $T=150^\circ\text{C}$ and were rotated during sputtering, to ensure composition uniformity. The magnetic metal volume fraction was controlled by the relative sputtering rates, and was then determined by energy-dispersive x-ray spectroscopy using a Philips EDAX XL30 on films deposited in the same run on Kapton tape. The samples deposited on Kapton tape were also used for magnetic measurements. Structural characterization was performed with TEM using a JEOL JEM-3010 microscope. Dc magnetization was measured on a Quantum Design MPMS XL7 system in the temperature range $5\text{--}380\text{ K}$ and fields up to 7 T . Ac susceptibility $\chi(T)$ measurements were done using the Quantum Design physical property measurement system in the available frequency range $10\text{--}10^4\text{ Hz}$. The susceptibility was measured in an ac magnetic field of 10 Oe after cooling the film in zero field. The ZFC procedure was repeated for each frequency and in the temperature range $5\text{--}300\text{ K}$.

IV. RESULTS AND DISCUSSION

Figure 1 shows the ZFC/FC data obtained on the $\text{Co}_x(\text{SiO}_2)_{1-x}$ films ($x=0.35, 0.41,$ and 0.44). Notice that the peaks in the ZFC curves, related to the mean blocking temperature, shift towards higher temperatures as the concentration x increases, indicating a continuous increase in the average grain size. It is noted that the ZFC/FC curves bifurcate at a temperature very close to the peak position for all samples. According to the noninteracting model presented in Sec. II, this would be the sign of a narrow distribution of blocking temperatures, and therefore of particle sizes, and

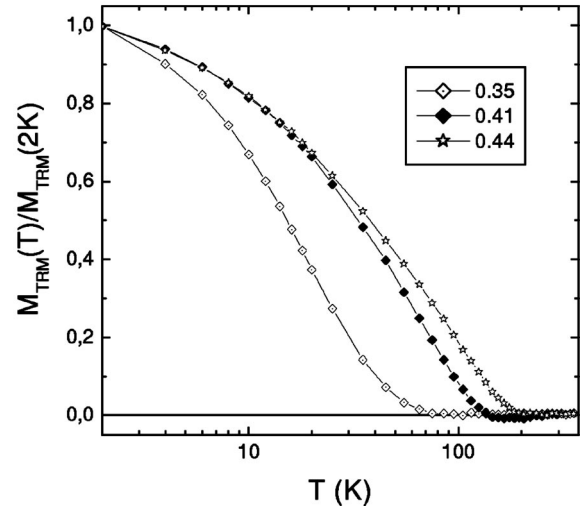


FIG. 2. Thermoremanent magnetization (TRM) curves, normalized to the values at $T=2\text{ K}$, for granular $\text{Co}_x(\text{SiO}_2)_{1-x}$ films with $x=0.35, 0.41,$ and 0.44 .

the maximum of the ZFC curve would correspond to the average blocking temperature. Figure 2 shows the results of TRM experiments, performed on the same set of samples (notice the logarithmic scale on the T axis). The curves resemble clearly the sigmoidal curve expected for a well-behaved superparamagnetic system, with the inflection point corresponding to the typical blocking temperature of the system. However, one immediately sees that the average blocking temperatures that would be deduced from the two kinds of measurements, ZFC/FC and TRM, are in total disagreement. Actually it was found impossible to fit both results to the above-quoted equations using the same distribution of (T_B). In order to further understand this behavior, we concentrated our efforts on the $\text{Co}_{0.35}(\text{SiO}_2)_{0.65}$ film, that has the lowest magnetic grain concentration, and on smaller grain sizes.

Figure 3(a) shows a cross-sectional TEM bright field image and dark field image [Fig. 3(b)] of an as-prepared granular film with $x=0.35$. The bright field image displays a microstructure characteristic of typical granular metal films, containing small metallic particles nearly spherical in shape. The dark field TEM images were taken by selecting a quarter of the strong diffraction rings, hence only the grains satisfying the selected diffraction conditions appear bright. The particle size histogram, shown in Fig. 4, was determined from several dark field TEM images, over a total number of 800 particles. The histogram was fitted using a log-normal distribution of particle diameters,

$$f(D) = \frac{1}{\sqrt{2\pi\sigma_D^2}} \frac{1}{D} \exp\left(-\frac{\ln^2\left(\frac{D}{\langle D \rangle}\right)}{2\sigma_D^2}\right), \quad (6)$$

from which we obtained the median particle diameter $\langle D \rangle = 3.2\text{ nm}$ and the distribution width $\sigma_D = 0.43$. Assuming a spherical particle shape the log-normal diameter distribution corresponds to a log-normal distribution of particle volume

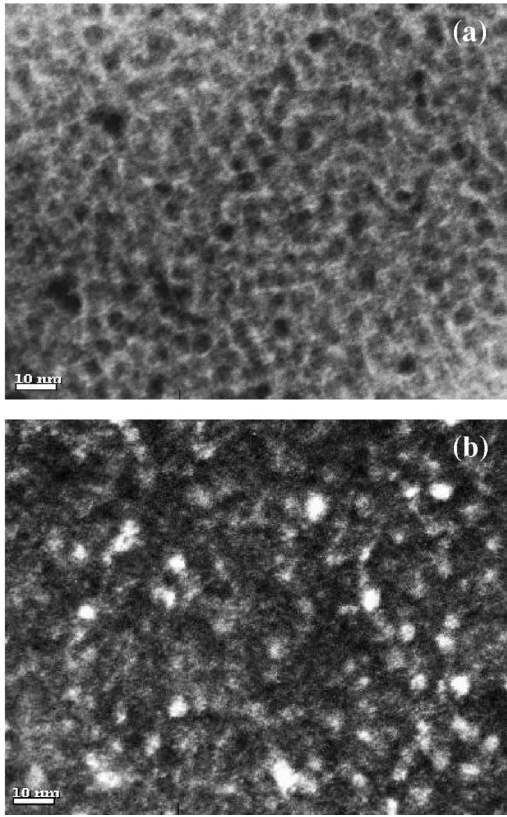


FIG. 3. Cross-sectional TEM bright field image (a) and dark field image (b) of the as-prepared granular film with metal volume fraction $x=0.35$.

with a median value $\langle V \rangle = (\pi/6)\langle D \rangle^3$ and a dispersion $\sigma_V = 3\sigma_D = 1.3$. Here and throughout the paper we use $\langle x \rangle$ to denote the median of a distributed variable x .

Using the model for ZFC/FC and TRM curves for noninteracting particles, we have fitted the experimental curves to Eq. (2) and (4). The result for ZFC/FC curves is shown as a solid line in Fig. 5 for the $\text{Co}_{0.35}(\text{SiO}_2)_{0.65}$ sample. The best fit was obtained using $\langle T_B \rangle = 51.3$ K and $\sigma = 0.25$. Figure 6 shows the corresponding blocking temperature distribution

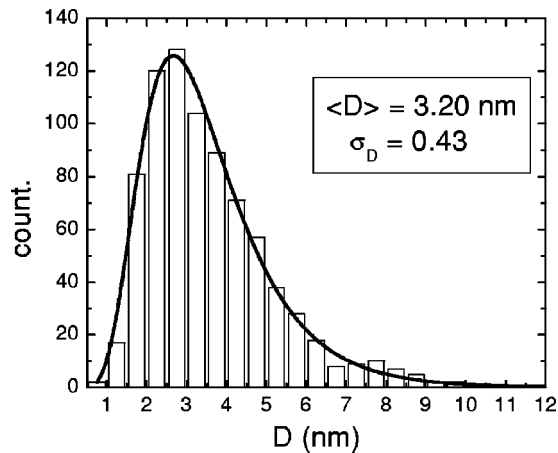


FIG. 4. Particle size histogram (bars) obtained from several dark field TEM images and adjusted by a log-normal curve (solid line).

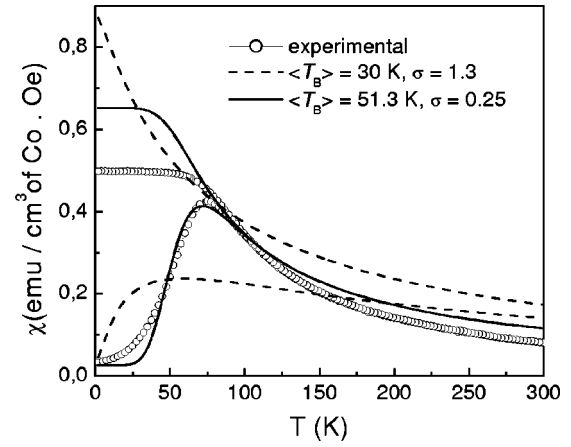


FIG. 5. Experimental ZFC/FC curve for the $\text{Co}_{0.35}(\text{SiO}_2)_{0.65}$ sample (symbols) and theoretical curve assuming a log-normal distribution with $\sigma=1.3$ and $\langle T_B \rangle = 30$ K (dashed line). The fit (solid line) of the experimental curve using the model described in the text gives $\langle T_B \rangle = 51.3$ K and $\sigma = 0.25$.

obtained from the derivative $d[M_{\text{ZFC}} - M_{\text{FC}}]/dT$ of the experimental data. This distribution was fitted to a log-normal one, from where we obtained $\langle T_B \rangle = 53.7$ K and $\sigma = 0.32$, in good agreement with the values obtained by fitting directly the ZFC/FC curves. Note that the fits in Figs. 5 [Eq. (2) and (4)] and 6 (log-normal distribution) do not match exactly the experimental data, but they are the best ones within the noninteracting superparamagnetic model.

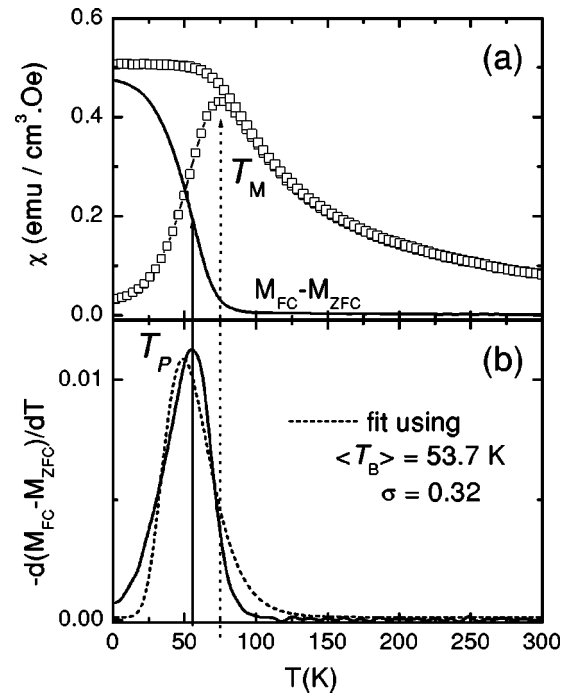


FIG. 6. (a) Experimental ZFC/FC curve for the $\text{Co}_{0.35}(\text{SiO}_2)_{0.65}$ sample (symbols) and the difference $M_{\text{FC}} - M_{\text{ZFC}}$ (solid line). (b) Blocking temperature distribution obtained from the derivative $d[M_{\text{ZFC}} - M_{\text{FC}}]/dT$ of the experimental data (solid line) adjusted by a log-normal distribution function (dashed line), from where we obtained $\langle T_B \rangle = 53.7$ K and $\sigma = 0.32$.

Both analyses show a much narrower distribution of blocking temperatures than expected from the real volume distribution ($\sigma_V = 1.3$). In addition the experimental value of $\langle T_B \rangle$ (≈ 54 K) is larger than the value ($\langle T_B \rangle \approx 30$ K) estimated using the median particle volume obtained from the TEM analysis, a typical value ($K = 6 \times 10^6$ ergs/cm³) for the uniaxial anisotropy constant of bulk hcp cobalt, and the time constants $\tau_0 = 10^{-9}$ s and $t_m = 100$ s. For comparison, Fig. 5 displays the expected ZFC/FC curves, which are in complete disagreement with the experimental ones. In particular the bifurcation between the simulated FC and ZFC curves occurs at a much higher temperature than that of the maximum ZFC curve, which is a consequence of the broad distribution of the actual particle sizes. As a matter of fact the difference between the experimental and expected values of $\langle T_B \rangle$ could be explained by an anisotropy constant larger than that of bulk Co, due, for instance, to interface effects with the SiO₂ matrix. However the much narrower distribution of T_B stresses the fact that the model of noninteracting particles simply does not apply to the present case. Most probably the effect of the size distribution is hidden by the overall effect of dipolar interactions that couple several neighboring particles.¹⁵

Indeed, the dipolar interaction among particles introduces a self-averaging effect over some interaction/correlation length Λ , which can obviously explain the narrower distribution of the “magnetic” sizes. Let N be the average number of particles contained within the correlation volume Λ^3 ; probability theory tells us that the volume fluctuations of the magnetic clusters of interacting particles (“particle clusters” or “superparticles” composed of magnetically coupled true particles) will be reduced by $N^{1/2}$. In addition, the “central limit theorem”¹⁴ tells us that the distribution of the cluster volumes should be more Gaussian-like, which is actually observed. From the ratio between the experimental dispersion of T_B ($\sigma_T \approx 0.25$) and the experimental dispersion of the particle volumes ($\sigma_V \approx 1.3$) one obtains $N = (\sigma_V / \sigma_T)^2 \approx 25$. Correspondingly, the average magnetic volume of the “particle clusters” will be N times larger than that of the physical ones. At first glance this would imply a blocking temperature 25 times larger than the expected 30 K for the average physical particle, whereas the measured $\langle T_B \rangle \approx 52$ K is only 1.7 times larger. The reasons for this apparent disagreement are twofold. First, if the particles are interacting, one cannot compare directly the observed value of $\langle T_B \rangle$ with that of the free particles since the relaxation times may differ considerably in the two cases. Second, the averaging effect of the interaction also modifies the effective anisotropy of the cluster and the effective energy barrier. Within the so-called random anisotropy model,^{16–18} the effective anisotropy constant in the volume Λ^3 is reduced by a factor $K_{eff}/K = x/N^{1/2}$, where x is the volume fraction of the magnetic particles. Therefore if our clustering model is correct we expect the average energy barrier for the “particle clusters” to be $K_{eff}\Lambda^3 = K(x/N^{1/2})(N\langle V \rangle/x)$, i.e., an increase, with respect to the isolated particle, by a factor $N^{1/2}$ only, i.e., 5 in our case.

In order to evaluate the relaxation time and the actual energy barrier, the temperature dependence of the ac suscep-

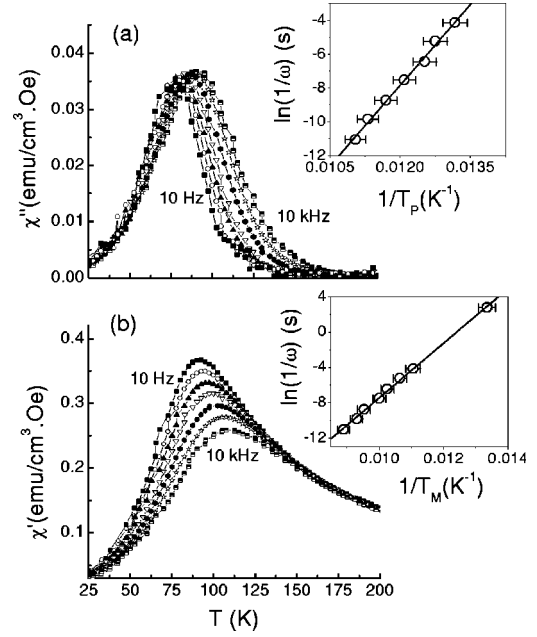


FIG. 7. Temperature dependence of ac susceptibility for the frequencies of 10, 30, 100, 300, 1000, 3000, and 10 000 Hz: (a) imaginary part $\chi''(T)$ and (b) real part $\chi'(T)$. Insets: (a) the plot of $\ln(1/\omega)$ vs $1/T_p$ for χ'' (symbols) and the linear fitting data (solid line), and (b) the plot of $\ln(1/\omega)$ vs $1/T_m$ (symbols), including the dc point for $t_m = 100$ s, and the linear fitting data (solid line).

tibility was measured in the frequency range 10–10⁴ Hz. Shown in Fig. 7 are the imaginary (χ'') and real (χ') components of ac susceptibility as functions of temperature for different frequencies. One can observe that the peaks in both $\chi''(T)$ and $\chi'(T)$ shift towards higher temperatures with increasing frequency of the ac field. The linear-response theory and Kramers-Kronig relations tell us that $\chi''(\omega, T)$ has a maximum when $\omega\tau = 1$, being $\omega = 2\pi f$ (f is the frequency of the ac field). Therefore, the frequency dependence of χ'' is commonly used to investigate the relaxation time and can be directly associated to the blocking temperature T_B .¹⁹ The inset of Fig. 7(a) shows the plot of $\ln(1/\omega)$ as a function of $1/T_p$, where the values of T_p , obtained from a Gaussian fit to the experimental curves, are the temperatures that correspond to the maximum of χ'' for each frequency (the error bars correspond to 2% in the determination of T_p). The plot displays that the blocking temperature does obey an exponential law showing thermal activation. However from a linear fit we deduce a value for the attempt frequency $1/\tau_0 \approx 10^{20}$ s⁻¹, which is without physical meaning for noninteracting nanoparticles.¹⁹ This excessively large value of the attempt frequency is again a clear indication of the important role of interparticle interactions in this system.²⁰ Although the real part of ac susceptibility does not peak exactly at T_B we have also plotted in Fig. 7(b) the frequency dependence of the temperature T_M where the maximum χ' occurs. In such an analysis, one can complement the parameters obtained from the ac susceptibility data with the ones obtained from the ZFC data, widening the frequency window from three orders of magnitude (in the case of the imaginary part) to six orders of magnitude (in the case of the real part). The

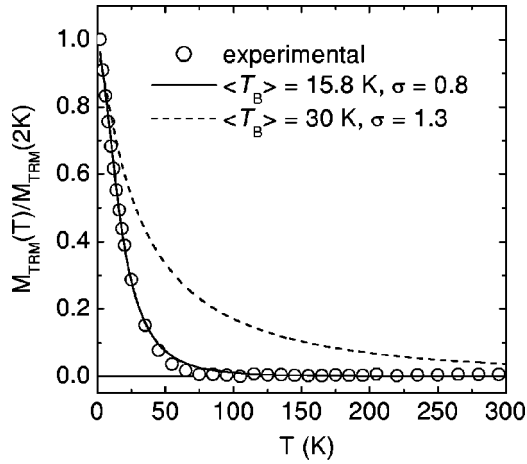


FIG. 8. Experimental TRM curve for the $\text{Co}_{0.35}(\text{SiO}_2)_{0.65}$ sample (symbols) and theoretical curve assuming a log-normal distribution with $\sigma=1.3$ and $\langle T_B \rangle=30$ K (dashed line). Adjusting the experimental curve with Eq. (5) we obtained $\langle T_B \rangle=15.8$ K and $\sigma=0.8$ (solid line).

plot of $\ln(1/\omega)$ as a function of $1/T_M$, as shown in the inset of Fig. 7(b) includes the dc measurement for $t_m=100$ s, and shows that the exponential behavior is indeed well obeyed over more than six decades.

From the linear fit, both sets of data show exactly the same slope from which we can infer the value of the energy barrier $\Delta E/k=3300$ K. This value is 4.4 times that computed for the median Co particle $K\langle V \rangle/k=750$ K in very good agreement with the value 5 predicted above. Actually the anisotropy constant of hcp Co lies in the range $K=5-7 \times 10^6$ ergs/cm³ and we could even find a perfect agreement using 5.3×10^6 ergs/cm³ instead of the tentative value of 6×10^6 ergs/cm³.

At this stage, we have shown that, without the structural information, our classical ZFC/FC measurements could be erroneously interpreted as arising from an assembly of non-interacting particles with a slightly larger volume and a much narrower size distribution than the actual ones. The frequency dependence of the susceptibility is thus essential for reconciliation of the existence of interactions. In particular, the attempt frequency for the relaxation can no longer be explained in the framework of Néel's theory. However, the other low-field properties have a behavior quite similar to that of independent particles, provided clusters of correlated particles are considered instead of single particles. Indeed, they are fully explained assuming clusters of N correlated particles and using the theoretical renormalization factor for random variables: the volume fluctuations are reduced by a factor $1/N^{1/2}$ while the energy barrier is increased by a factor $N^{1/2}$, with respect to noninteracting particles.

The effect of interactions is also evidenced from the experimental TRM curves, as shown in Fig. 8. Indeed, the experimental TRM starts decreasing at much lower temperature than that expected from the simple model. Adjusting the experimental curve to Eq. (5) we obtained $\langle T_B \rangle=15.8$ K and $\sigma=0.8$. Hence, contrary to the case of ZFC/FC curves, the experimental TRM curve would suggest a blocking tempera-

ture two times lower than the expected 30 K and 3.5 times lower than the FC/ZFC measurements. On the other hand, it must be pointed out that a blocking temperature of $\langle T_B \rangle=15$ K, as observed, would be predicted using the energy barrier of the single average particle together with the actual value of τ_0 found for the clusters. We tend to believe that the latter agreement is fortuitous. Indeed it does not seem consistent to attribute to a single-particle relaxation process the attempt frequency found for clusters of correlated particles. However this observation points towards a more individual behavior of the relaxation process from the magnetized state. The larger distribution width of T_B that is deduced from the TRM curve also supports the claim. It is still lower than expected from the size histogram, though.

Actually, the “particle clusters” can be considered as “domains,” inside which the orientation of the particle moments are highly correlated (not parallel, though), separated by “walls” where the dipolar interaction is more frustrated. The low-field susceptibility measurements probe a collective response of the particles within the clusters with only weak relative reorientation between the particle moments. The TRM differs from the other kinds of measurement since it starts from a state where all the moments are nearly aligned along the strong applied field. Then, when the field is removed, the relaxation can occur through “domain” nucleation and “wall” formation, while, for the measurements in weak field, domainlike structures are always present in the sample. Therefore the relaxation process from the saturated state to the zero-field state(s) involves both collective rearrangements of the cluster moments and large rearrangements of the individual moments within the clusters.

Along this line of thought one can tentatively compare the thermal demagnetization process to the field-induced reversal process at low temperature. For a single domain particle the coercive field at 0 K is equal to the saturation field and equal to the anisotropy field. For hcp Co this coercive field is about 8 kOe along the easy axis and for a powder average (random orientation) it is around 4 kOe. In our sample the coercive field at 2 K, well below the blocking temperature, is 2.2 kOe, which is approximately two times lower than expected. This is in good agreement with the reduction of the average demagnetizing temperature as measured by TRM with respect to the blocking temperature of individual particles.

These observations suggest that we are observing the beginning of the formation of a collective magnetic state arising from the dipolar interactions among individual particles.²¹ Such magnetic ordering has been called “superferromagnetism” in cases where the dipolar interaction leads to ferromagnetic coupling between the magnetic objects.^{22,23} In our case, the distribution of sizes and distances implies a distribution of the strength and the orientation of the interaction, which would rather lead to a “cluster spin-glass-like” state. However the average blocking temperature is higher than the freezing temperature of the hypothetical spin-glass transition²⁴ since the correlation length due to the interaction is still quite small around the blocking temperature. This is probably why the weak-field properties can still be reasonably described in the framework of independent “particle

clusters” after a renormalization taking into account the correlation length. On the other hand, the renormalization does not apply to the thermal demagnetization process from a saturated state where individual relaxation must also take place.

V. CONCLUSION

We have studied Co(SiO₂) granular films by means of dc and ac initial susceptibility and thermoremanent magnetization. The sample with metal volume fraction $x=0.35$ has been studied in more detail, including a complete structural characterization by means of TEM in order to obtain the real size distribution of the magnetic particles. Using a simple model of noninteracting superparamagnetic particles, we have shown that important parameters such as median blocking temperature and size distribution of particles deduced from the analysis of the ZFC/FC and TRM curves differ substantially, both being very different from the values obtained from the direct structural analysis. We conclude that the dipolar interaction among particles introduces a self-averaging effect over some correlation length Λ , that results in a larger average “magnetic” size of the apparent particles together with a narrower size distribution. Indeed the FC/ZFC curves can still be analyzed in the framework of independent clusters of particles of volume Λ^3 , involving around 25 real particles in our case. Such renormalization predicts very well the observed difference between the experimental data for the average blocking temperature $\langle T_B \rangle$ and its distribution width with respect to the ones expected from the structural observations by TEM. On the other hand, the temperature dependence of the TRM shows a quite different behavior from that of the ZFC/FC curves, with a much smaller apparent blocking temperature. This result cannot be explained in terms of independent particles, renormalized or not. We concluded that the magnetic relaxation processes during the TRM measurement, which starts from a magne-

tized state, mixes both collective (between clusters) and individual (within clusters) demagnetizing process involving energy barriers smaller than that for the magnetization reversal of a single particle. In other words, the decay from the fully magnetized state is mostly driven by the anisotropy of the individual particles and their coupling, while the energy barrier deduced from low-field measurements is that from the reorientation of the “superparticles.” Generally speaking, extreme care must be paid when dealing with nanomagnets, because the dipolar interaction among them can play a fundamental role in the overall magnetic behavior, even at relatively low magnetic element concentrations. These results are particularly important if one wants to obtain indirect structural information through magnetic measurements, because a single experiment can lead to incorrect estimates of mean grain sizes and their distribution. Owing to the dipolar magnetic interactions, the nanocrystalline system macroscopically behaves as composed of larger grains with a narrow dispersion. As a matter of fact, the most common experimental curves remain very similar to the ones expected for a noninteracting system, but with a different grain-size distribution. Having more experiments performed on the same sample will make it possible to check for the existence or absence of interactions, and, in principle, renormalize the results in order to obtain the true nanostructure and properly estimate the effect of dipolar interactions.

ACKNOWLEDGMENTS

This work was financially supported by FAPESP and CNPq (Brazilian agencies). The TEM images were performed at the Laboratório de Microscopia Eletrônica (LME - LNLS), Campinas, Brazil. H. Liu and X.X. Zhang acknowledge the support of the research grants of the Hong Kong Special Administrative Region, China (Project No. HKUST 6159/99P).

-
- ¹A.E. Berkowitz, J.R. Mitchell, M.J. Carey, A.P. Young, S. Zhang, F.E. Spada, F.T. Parker, A. Hutten, and G. Thomas, *Phys. Rev. Lett.* **68**, 3745 (1992).
- ²J.Q. Xiao, J.S. Jiang, and C.L. Chien, *Phys. Rev. Lett.* **68**, 3749 (1992); *Phys. Rev. B* **46**, 9266 (1992).
- ³T. Jonsson, J. Mattsson, C. Djurberg, F.A. Khan, P. Nordblad, and P. Svedlindh, *Phys. Rev. Lett.* **75**, 4138 (1995).
- ⁴W. Luo, S.R. Nagel, T.F. Rosenbaum, and R.E. Rosensweig, *Phys. Rev. Lett.* **67**, 2721 (1991).
- ⁵J. García-Otero, M. Porto, J. Rivas, and A. Bunde, *Phys. Rev. Lett.* **84**, 167 (2000).
- ⁶E.F. Ferrari, F.C.S. da Silva, and M. Knobel, *Phys. Rev. B* **56**, 6086 (1997).
- ⁷M.F. Hansen and S. Mórup, *J. Magn. Magn. Mater.* **203**, 214 (1999).
- ⁸P. Panissod, M. Malinowska, E. Jedryka, M. Wojcik, S. Nadolski, M. Knobel, and J.E. Schmidt, *Phys. Rev. B* **63**, 014408 (2001).
- ⁹A.B. Pakhomov, X. Yan, and B. Zhao, *Appl. Phys. Lett.* **67**, 3497 (1995).
- ¹⁰J.C. Denardin, A.B. Pakhomov, M. Knobel, H. Liu, and X.X. Zhang, *J. Phys.: Condens. Matter* **12**, 3397 (2000).
- ¹¹L. Néel, *Ann. Geofis.* **5**, 99 (1949).
- ¹²E.P. Wohlfarth, *Phys. Lett. A* **70**, 489 (1979).
- ¹³R.W. Chantrell, M. El-Hilo, and K. O’Grady, *IEEE Trans. Magn.* **27**, 3570 (1991).
- ¹⁴J. R. Taylor, *An Introduction to Error Analysis: The Study of Uncertainties in Physical Measurements*, 2nd ed. (University Science Books, Sausalito, 1997).
- ¹⁵S. Sankar, D. Dender, J.A.S. Borchers, D.J. Smith, R.W. Erwin, S.R. Kline, and A.E. Berkowitz, *J. Magn. Magn. Mater.* **221**, 1 (2000); S. Sankar, A.E. Berkowitz, and D.J. Smith, *Phys. Rev. B* **62**, 14 273 (2000).
- ¹⁶G. Herzer, *IEEE Trans. Magn.* **25**, 3327 (1989).
- ¹⁷G. Herzer, *IEEE Trans. Magn.* **26**, 1397 (1990).
- ¹⁸A. Hernando, M. Vázquez, T. Kulik, and C. Prados, *Phys. Rev. B* **51**, 3581 (1995).
- ¹⁹X.X. Zhang, G. Gu, H. Huang, S. Yang, and Y. Du, *J. Phys.:*

- Condens. Matter **13**, 3913 (2001).
- ²⁰J.L. Dormann, F. D’Orazio, F. Lucari, E. Tronc, P. Prené, J.P. Jolivet, D. Fiorani, R. Cherkaoui, and M. Nogues, Phys. Rev. B **53**, 14 291 (1996).
- ²¹P. Allia, M. Coisson, M. Knobel, P. Tiberto, and F. Vinai, Phys. Rev. B **60**, 12 207 (1999).
- ²²M.F. Hansen, C.B. Koch, and S. Mørup, Phys. Rev. B **62**, 1124 (2000).
- ²³J. Hauschild, H.J. Elmers, and U. Gradmann, Phys. Rev. B **57**, R677 (1998).
- ²⁴S. Mørup, F. Bødker, P.V. Hendriksen, and S. Linderoth, Phys. Rev. B **52**, 287 (1995).